

Study on Explosion Characteristics and Mechanism of Electrostatic Spray Powder

Xinxin Qin, Yansong Zhang, Jing Shi, and Xiangrui Wei*

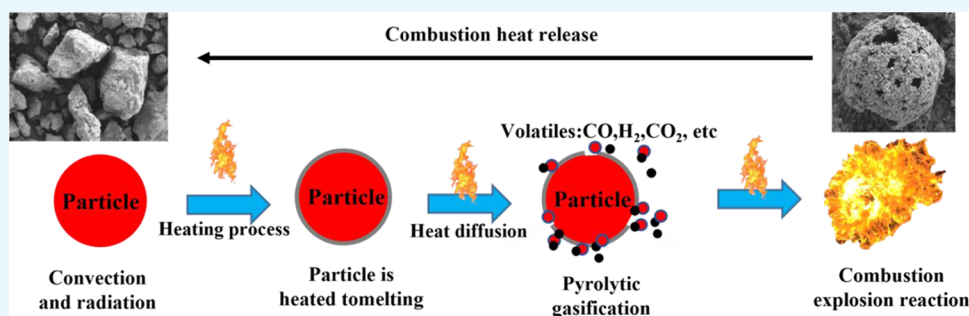
Cite This: *ACS Omega* 2024, 9, 19645–19656

Read Online

ACCESS |

Metrics & More

Article Recommendations



ABSTRACT: In order to fully understand the explosion risk of electrostatic spraying powder, corresponding preventive measures are put forward. The explosion characteristics, ignition sensitivity, and flame propagation of three typical electrostatic spraying powders were tested using a 20 L spherical explosion test device, a G–G furnace test device, and a Hartmann tube test device, and the explosion process and mechanism of electrostatic spraying powders were discussed. The results show that the maximum explosion pressure and the maximum explosion pressure rise rate increase first and then decrease with the increase in mass concentration. The maximum explosion pressure and the maximum explosion pressure rise rate of acrylic powder coating are the largest, which are 0.75 and 85.4 MPa/s, respectively. The shortest burning time is 97.5 ms, and the highest explosion danger level is 23.46 MPa·m/s. The flame propagation of electrostatic spraying powder develops slowly; the flame front spreads linearly and the average flame velocity increases first and then decreases. The explosive development process of powder coating particles is concentrated in the three-phase system of solid particles, molten particles, and pyrolytic gasification combustible gas, which goes through the kinetic process of particle heating melting, cross-linking curing, pyrolytic gasification, combustion, and extinction.

1. INTRODUCTION

Electrostatic spraying is a surface coating technology based on the principle of static electricity. It utilizes the corona discharge of electric field strength and aerodynamic force to make powder coating particles negatively charged under the action of high-voltage direct current electric field and adsorb on the positively charged substrate surface.¹ Among them, epoxy, polyester, and acrylic powder coatings have the advantages of good leveling, fast film formation and good coloring power, and become the three typical electrostatic spraying powders with the largest use.² The demand for these three powder coatings is increasing in industries, such as construction, automotive manufacturing, aerospace manufacturing, and electronics. However, the main raw materials for electrostatic spraying are combustible substances such as polyurethane and epoxy resin, and during the electrostatic spraying process, dust tends to accumulate and suspends in relatively enclosed and confined spaces,³ posing a certain risk of dust explosion. Therefore, in order to understand the explosion risk of electrostatic spraying powder and take effective explosion prevention measures, it is particularly

important to study the explosion of electrostatic spraying powder.

At present, there are many pieces of research on dust explosion, mainly focusing on common combustible dust such as metal powder^{4–6} and coal powder.^{7–9} Millogo et al.¹⁰ used the Hartmann tube and 20 L spherical explosive tank to study the minimum ignition energy, explosion pressure, and explosion pressure rise rate of Al powder and part of Al alloy powder. Jiang et al.¹¹ developed a new type of chemical inhibitor and studied its inhibitory effect on Al powder. The results indicate that adding 33% of a new chemical inhibitor can completely suppress the explosion of nano-Al powder. Liu et al.¹² studied the inhibitory effect of different proportions of $\text{Ca}(\text{H}_2\text{PO}_4)_2$ and

Received: February 22, 2024

Revised: March 20, 2024

Accepted: April 3, 2024

Published: April 16, 2024



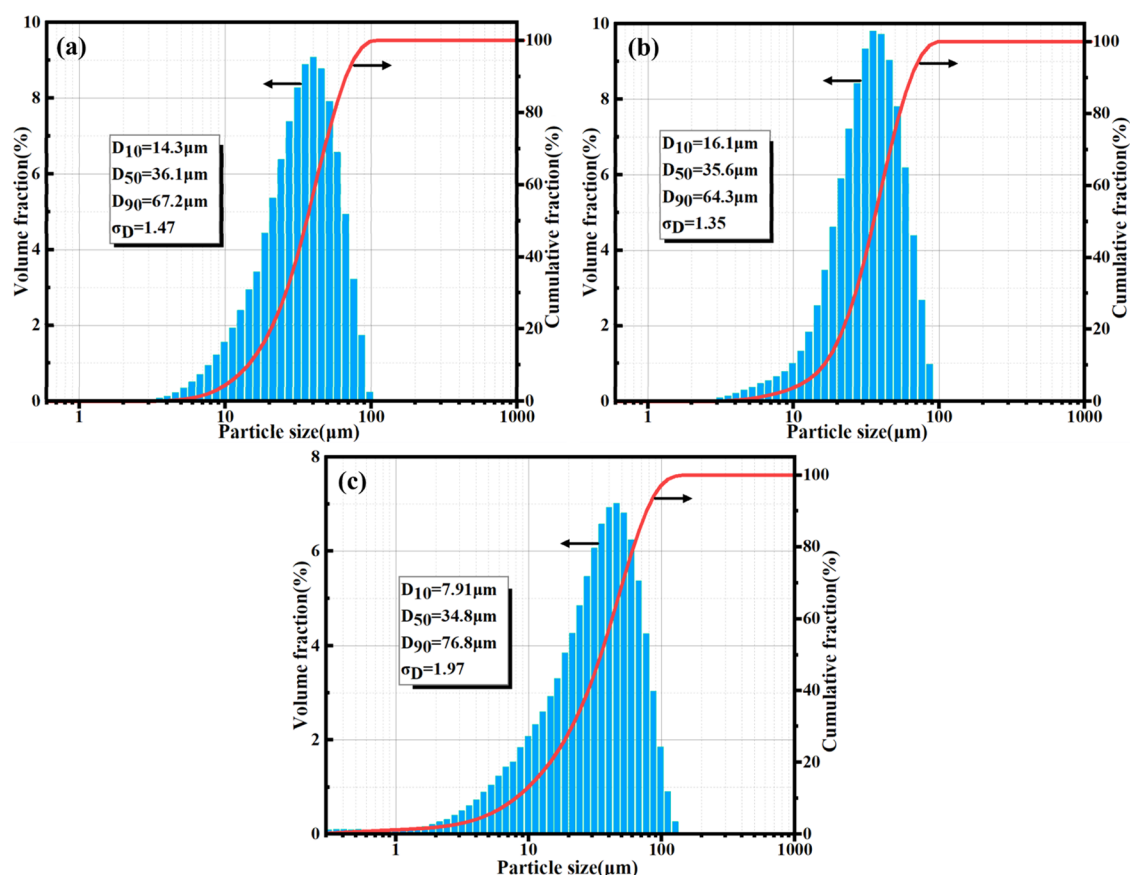


Figure 1. Particle size distribution of electrostatic spraying powder samples. (a) Epoxy powder coating. (b) Polyester powder coating. (c) Acrylic powder coating.

CaCO_3 powders on the explosion of Ti powder using Hartmann and 20 L spherical explosive tank devices. The experiment showed that both $\text{Ca}(\text{H}_2\text{PO}_4)_2$ and CaCO_3 had a certain inhibitory effect on the explosion of the Ti powder. Huang et al.¹³ studied the inhibitory effect of ultrafine $\text{Mg}(\text{OH})_2$ powders with different particle sizes and mass fractions on the explosion flame of sawdust, and the results showed that nanoscale $\text{Mg}(\text{OH})_2$ had a better inhibitory effect on sawdust. Liu et al.¹⁴ proposed the inhibition mechanism of NaHCO_3 on oil shale using thermogravimetric differential scanning calorimetry combined with scanning electron microscope (SEM) images of explosive residues. Zhao et al.¹⁵ designed a N_2/APP two-phase explosion suppression system, which suppresses the explosion after the explosion, rather than pre-mixing and inerting the explosive medium. Compared to electrostatic spraying powder, it has received less attention. At present, research on electrostatic spraying powder mostly focuses on improving process equipment and optimizing the performance of powder coatings,^{16,17} and only a few scholars have conducted preliminary discussions on the explosive properties of spraying materials. Li et al.¹⁸ found that powder coatings have explosive properties, with ignition energy higher than ordinary dust such as coal powder and corn starch. They proposed protective measures mainly based on explosion isolation and venting. Bielawski¹⁹ elaborated on the hazards and combustion characteristics of electrostatic powder coatings and provided recommendations for the safety protection of spraying devices. Di Benedetto and Russo²⁰ developed software for calculating the thermal dynamics of dust explosions and calculated the deflagration index and the laminar combustion rate of a series of organic dust,

including electrostatic powder coatings. Velicka et al.²¹ showed that the clear division of areas with explosion risk into different areas is the basis for determining the degree of preventive measures in these areas. Incorrect classification of hazardous areas can lead to a lack of clarity on the extent of protective measures. Eckhoff et al.²² studied the explosive properties of polyester/epoxy resin powder by using 1.2 L Hartmann tube and believed that the combustion of organic pigments in the powder might help to increase the explosion pressure.

At present, the research on the explosive characteristics of electrostatic spraying powder is still in the exploratory stage, people do not know much about the explosion risk of electrostatic spraying powder, and the combustion dynamics and explosion characteristics data of electrostatic spraying powder are insufficient, which makes it difficult to provide effective data support for the explosion safety protection of enterprises. In order to understand the explosion risk of electrostatic spraying powder more clearly, three typical electrostatic spraying powder coatings, epoxy powder coating (EPC), polyester powder coating (PPC), and acrylic powder coating (APC), were taken as the research object. The explosion characteristic parameters, ignition sensitivity parameters, and flame propagation characteristics of three powder coatings were studied using the 20 L spherical explosion system, the Godbert–Greenwald furnace experimental system, and the Hartmann tube experimental system. By observing the microscopic characteristics of particles before and after the explosion, the explosion mechanism of electrostatic spraying powder was analyzed, which is helpful for the production and application of electrostatic spraying powder. The prevention and control of

explosion accidents during storage, transportation, and application provide important data reference and theoretical basis.

2. EXPERIMENTAL SECTION

2.1. Preparation and Characterization of Experimental Samples. The EPC, PPC, and APC used in the experiment were purchased from Zhongshan Hongli Mei New Materials Technology Co., Ltd., which are mainly composed of resin, pigment, filler, and additives. At first, the sample was placed in a vacuum drying oven and dried at 50 °C to ensure that the moisture content of the powder sample was less than 5%. Then, a 200 mesh sieve was used to screen the three powder coatings separately. The particle size distribution of the screened powder samples was characterized using the Mastersizer 2000 laser particle size analyzer from Marvin Instruments Limited in the U.K. Statistical diameters D_{10} , D_{50} , and D_{90} were given, and the particle size dispersion (σ_D) used to characterize the particle size distribution span was calculated using eq 1²³ as shown in Figure 1. The results showed that the median particle size D_{50} of EPC, PPC, and APC was 36.1, 35.6, and 34.8 μm , respectively. Particle size dispersion σ_D values were 1.47, 1.35, and 1.97, respectively. The particle size distribution area of the three powder samples was relatively narrow, and the particle size distribution was relatively concentrated, with similar D_{50} values and σ_D . This prevented the impact of powder particle size on the experimental results.

$$\sigma_D = (D_{90} - D_{10})/D_{50} \quad (1)$$

Thermogravimetric analysis (TGA) is an important method for studying the pyrolysis characteristics of dust particles.^{24,25} The thermal decomposition characteristics of three powder particles in an air atmosphere were measured using an STA PT 1600 synchronous thermal analyzer and thermogravimetric analyzer from Lindeis, Germany. The heating rate was set at 10 °C/min, and the temperature range was 25 to 800 °C. Figure 2 shows the TG curves of three powder samples, and there is no significant change in the TG curves at low temperatures below 240 °C. This is mainly because the samples were dried before the experiment, and the moisture content in the samples was very low. The moisture loss during the low-temperature heating stage was minimal. As the temperature increased, the mass of all three

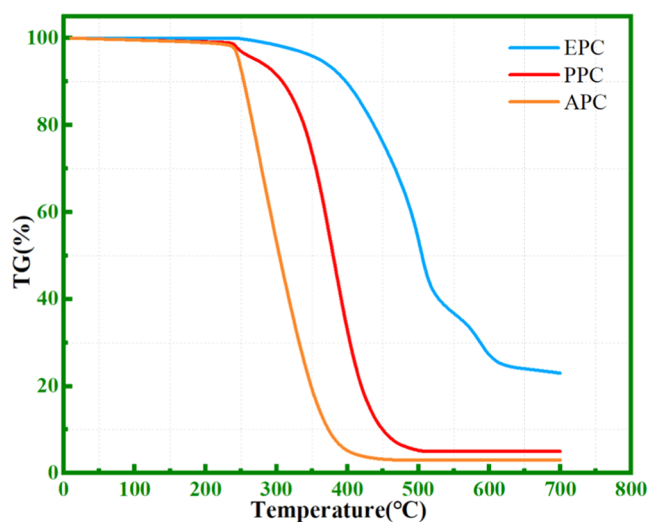


Figure 2. TG curve of electrostatic spraying powder samples.

samples began to significantly decrease. APC began to lose mass earlier than the other two powders, with the lowest mass loss temperature (240 °C), and the mass loss rate reached its maximum value within the temperature range of $T = 370\text{--}410$ °C. In contrast, EPC has the highest mass loss temperature (360 °C) and the slowest particle thermal decomposition rate. After $T > 600$ °C, the TG curves of EPC, PPC, and APC all tend to be flat, with no mass loss, and mass loss rates reaching 75.6, 95.5, and 97.8%. This indicates that under the same heating conditions, APC has the highest volatile content, followed by PPC and EPC.

The surface morphology of the electrostatic powder coating before and after explosion was observed with an electron scanning microscope (Zeiss Gemini 300) produced by Carl Zeiss GMBH.

2.2. Explosion Characteristic Experiment. The explosion characteristics of the three typical electrostatic spraying powders EPC, PPC, and APC were tested in the 20 L spherical explosion experimental device produced by Jilin Hongyuan Scientific Instrument Co., LTD, as shown in Figure 3. Before the experiment, according to the “zero oxygen balance” rule, an ignition charge head was made by mixing 30% barium nitrate, 30% barium peroxide, and 40% zirconium powder by mass ratio. The ignition energy was 10 kJ, and the ignition charge head was installed on the ignition electrodes at both ends of the explosion tank. Then, a certain quantity of dust sample is placed in the powder storage tank and sealed. High-pressure air of 2 MPa is filled into the gas storage tank, and the vacuum pumping device is started to vacuum the explosion tank to -0.06 MPa. This achieves the experimental condition of the initial environmental pressure of the powder at the time of ignition being standard atmospheric pressure.^{26,27} Finally, the experimental program is initiated through the control system for the experiment, and the data collection system collects pressure data. After the action of the powder spraying system, the ignition system delays the ignition by 60 ms to ensure full diffusion of dust at the ignition time. After the experiment, the post-explosion products were collected, and the experimental equipment was cleaned to avoid affecting the accuracy of the next experimental data. In order to obtain reliable experimental results, each group of experiments was repeated 5 times, and the experimental data were averaged.

2.3. Ignition Sensitivity Test and Flame Propagation Experiment. The minimum ignition temperature (MITC) of dust clouds for three typical electrostatic spraying powders, epoxy, polyester, and acrylic was tested in the Godbert–Greenwald (G-G) furnace experimental setup produced by Jilin Hongyuan Scientific Instrument Co., Ltd. in China. The experimental device consists of a heating furnace, a dust storage tank, a gas storage tank (0.5 L), a high-pressure gas storage bottle, and a temperature control system (with a temperature adjustment range of 25–1000 °C), as shown in Figure 4. The experiment was conducted according to the MITC test method for combustible dust clouds specified in the standard GB/T 3836.12–2019/ISO/IEC 80079–20:2:2016.^{28,29} During the experiment, a certain quantity of powder sample is first loaded into the dust storage tank and sealed, and the gas storage tank is pressurized to the set pressure through a high-pressure gas storage bottle. Then the heating furnace was turned on to raise the temperature. Start the experiment after the temperature inside the heating furnace reaches the preset ignition temperature. Spray the powder sample into the heating furnace through high-pressure air and observe if the dust cloud catches

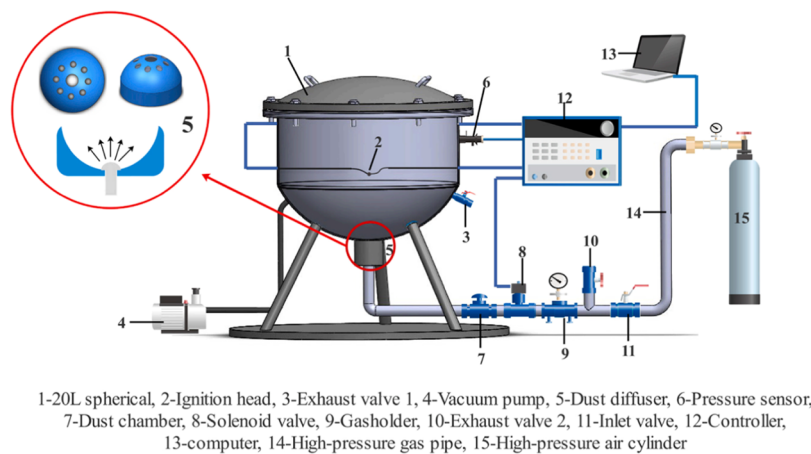


Figure 3. 20 L spherical explosion test apparatus.

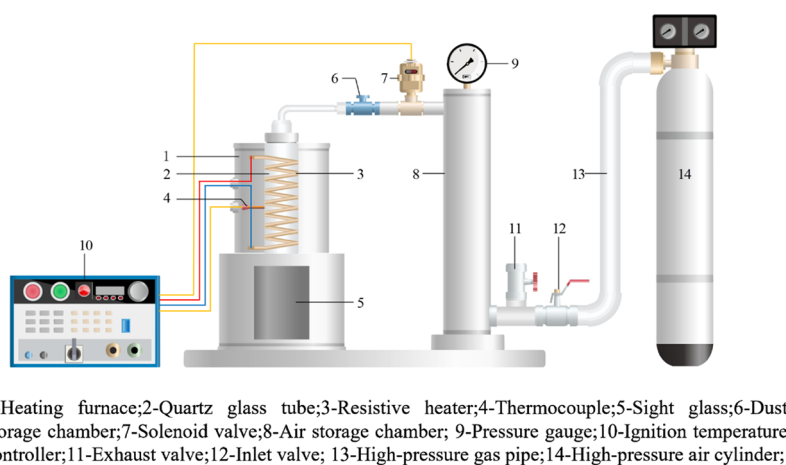


Figure 4. Godbert–Greenwald (G-G) furnace.

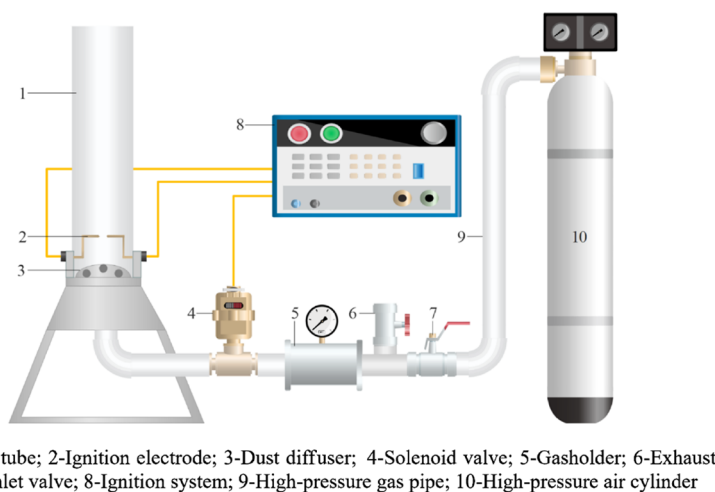


Figure 5. Hartmann tube experimental device.

fire. According to the ignition situation of the dust cloud, by changing the quality of the powder sample, ignition delay time, and air dispersion pressure, the ignition temperature gradually reduced until no ignition occurred in 10 repeated tests. Then, 20 °C was subtracted from the previous ignition temperature value to determine the MITC value of the powder sample.

The dust cloud minimum ignition energy (MIE) of three typical electrostatic spraying powders, epoxy, polyester and acrylic was tested in the Hartmann tube experimental equipment produced by Jilin Hongyuan Scientific Instrument Co., LTD.^{30,31} The experimental device consists of a vertical transparent quartz glass tube (1.2 L), an air storage tank, a dust dispersion device, an ignition energy generator, and a high-

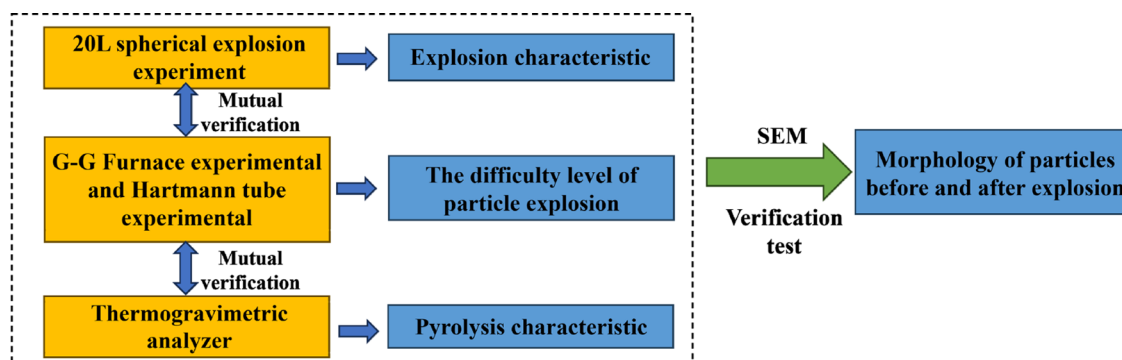


Figure 6. Experimental flowchart.

pressure gas storage cylinder, as shown in Figure 5. The experiment was conducted according to the MIE testing method for dust/air mixtures specified in the standard GB/T 3836.12–2019/ISO/IEC 80079–20:2:2016. First, evenly place a certain quality of powder sample is evenly placed on the dust dispersion device at the bottom of the glass tube, and the gas storage tank is pressurized to the set pressure through a high-pressure gas storage bottle. Then, the ignition delay time was set, the ignition energy generator was adjusted to the required ignition energy value, and a certain concentration of dust cloud was formed in the glass tube with compressed air at the set pressure. Use electrode discharge ignition to observe whether the dust cloud in the tube is on fire and spreading. Based on the ignition situation, the quality of the powder sample, ignition delay time, and dispersion pressure were changed, the ignition energy was adjusted, and the experiment continued until no ignition occurred in 10 repeated tests. It is determined that the MIE of the dust sample is between the temperature at which no ignition occurs in 10 repeated tests and the temperature at which ignition occurs in 10 repeated tests. To study the flame propagation of three typical electrostatic spraying powders in vertical glass tubes, a high-speed camera was used to record the dynamic propagation process of flames in vertical glass tubes when the powder sample mass was 0.6 g and the ignition energy was 2J.

The correlation between the experiments described above is shown in Figure 6.

3. RESULTS AND DISCUSSION

3.1. Severity of Dust Cloud Explosion. The typical explosion pressure evolution curve obtained in a 20 L explosion test device is shown in Figure 7, and two important characteristic

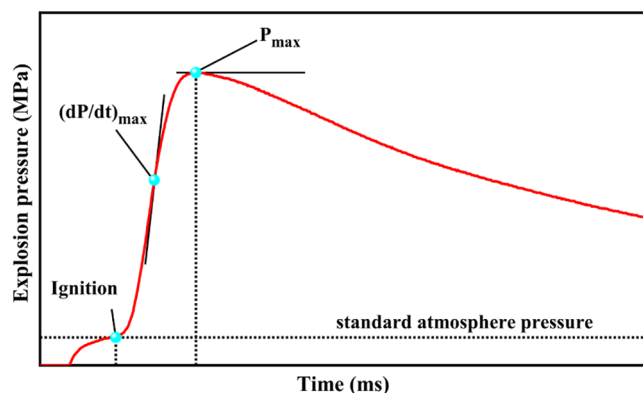


Figure 7. Typical explosion pressure evolution curve.

parameters used to evaluate the severity of dust explosion are marked in the figure: maximum explosion pressure (P_{\max}) and maximum explosion pressure rise rate ($(dP/dt)_{\max}$). The $(dP/dt)_{\max}$ of dust is closely related to the volume of the explosion container, but the explosion index (K_{st}) is a constant, represented by the product of $(dP/dt)_{\max}$ and the cube root of the explosion container volume, as shown in eq 2. Therefore, K_{st} is commonly used as an important parameter to measure the severity of dust explosions³².

$$K_{st} = \left(\frac{dp}{dt} \right)_{\max} \times V^{1/3} \quad (2)$$

Multiple sets of explosion characteristics tests were conducted on three powder coatings, EPC, PPC, and APC, at a mass concentration range from 250 to 1250 g/m³. According to the test results of the explosion characteristics parameters of three powder coatings, the maximum explosion pressure P_{\max} of the three powder coatings was conducted on three powder coatings, epoxy, polyether, and acrylic, at a mass concentration range of 250–1250 g/m³. According to the test results of the explosion characteristics parameters of the three powder coatings, the maximum explosion pressure P_{\max} of the three powder coatings is between 0.63 and 0.75 MPa, with APC > EPC > PPC. $(dP/dt)_{\max}$ is between 44.5 and 85.4 MPa/s, APC > EPC ≈ PPC, and APC reaches its peak at a mass concentration of 1000 g/m³. Figure 8 depicts the variation curves of P_{\max} and $(dP/dt)_{\max}$ with the mass concentration for the three powders. As shown in Figure 9a, the maximum explosion pressure of the three powder coatings shows a trend of first increasing and then decreasing with the increase in mass concentration. In the low concentration range (250 g–750 g/m³), an oxygen rich environment with sufficient oxygen content results in sufficient reaction. As the powder concentration increases, the number of effective particles participating in the reaction per unit space increases, the combustion rate accelerates, and the heat release increases, resulting in a rapid increase in the P_{\max} for all three types of dust. When a certain concentration is reached, the powder and oxygen reach the optimal mass concentration ratio, at which point the reaction is most complete, and P is maximum. In the high concentration range (750 g–1250 g/m³), incomplete combustion is formed inside the dust particles due to insufficient oxygen content, resulting in a decrease in the heat release rate of particle surface combustion. Additionally, unreacted dust particles absorb some of the combustion heat and reduce the heat release, resulting in a slow decrease in P_{\max} , showing an overall inverted “U” shaped change pattern. As shown in Figure 9b, $(dP/dt)_{\max}$ also exhibits a similar trend of

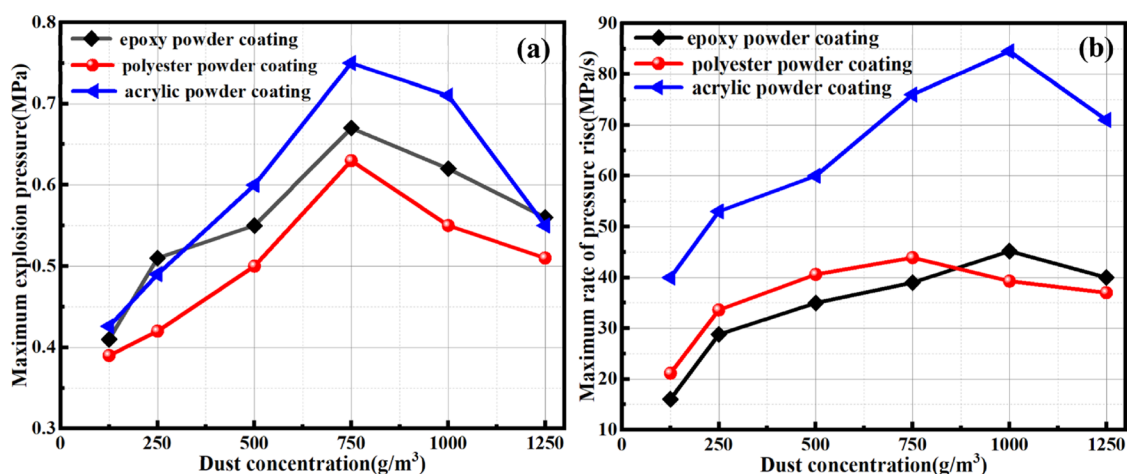


Figure 8. Relationship between P_{\max} and $(dP/dt)_{\max}$ of dust clouds and dust concentration: (a) P_{\max} ; (b) $(dP/dt)_{\max}$.

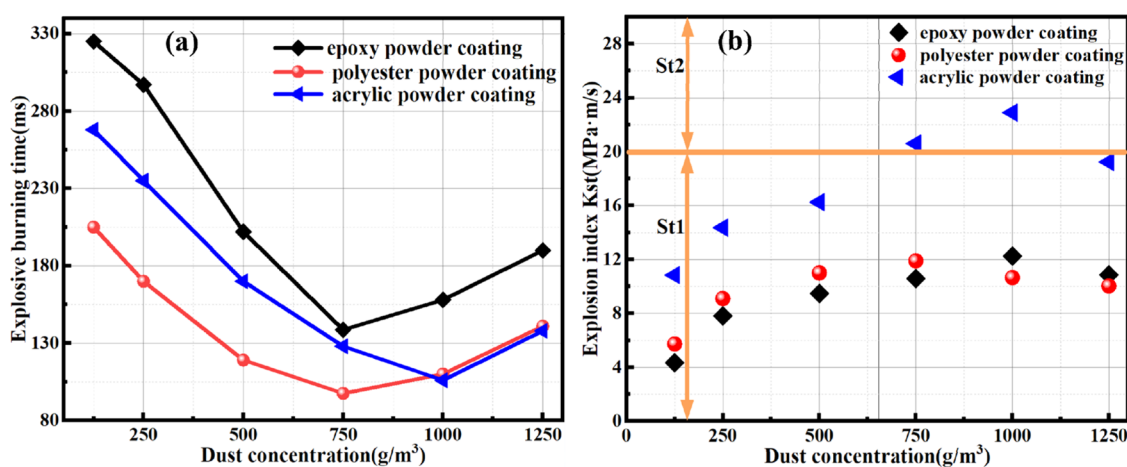


Figure 9. Relationship between T_b and K_{st} of dust clouds and dust concentration: (a) T_b ; (b) K_{st} .

change. In the initial stage, under the action of a high-temperature ignition source, dust particles first undergo pyrolysis to release volatile components, which rapidly oxidize and burn. Then, the gas-phase combustion flame continues to heat the surrounding unburned dust particles, further triggering the thermal decomposition of the powder coating particles. The rate of volatilization analysis is accelerated, and the content of volatile matter increases, leading to an acceleration of combustion reaction and a rapid increase in $(dP/dt)_{\max}$. But as the mass concentration continues to increase, the combustion rate will not always accelerate and will also be limited by oxygen content and heat loss, resulting in a decrease in $(dP/dt)_{\max}$, but the decrease is small and tends to stabilize.

The dust combustion time T_b refers to the time from the ignition moment to reaching the maximum explosion pressure. In the design of explosion suppression systems, T_b has an important reference significance for determining the reaction time of the device. As shown in Figure 9a, the combustion time of the three powder coatings is EPC > PPC > APC. The shortest combustion time of APC is 97.5 ms, while the longest combustion time of EPC is 138.6 ms, which is 41.1 ms more than that of APC. This is mainly because under the same heating conditions, APC has the highest organic volatile content and the lowest glass transition temperature T_g . The higher the volatile content, the easier it is to explode, and the faster the heat release rate of powder particle combustion, resulting in a shorter time to

reach the maximum explosion pressure. According to Figure 9b, from the maximum explosion index ($K_{st})_{\max}$ APC has the highest ($K_{st})_{\max}$ at 23.46 MPa·m/s, while EPC and PPC have little difference in ($K_{st})_{\max}$ at 10.73 and 10.81 MPa·m/s, respectively. According to the German explosion index classification method,³³ the explosion hazard levels for EPC, PPC, and APC are S_{t1} , S_{t1} , and S_{t2} , respectively. APC has the highest explosion hazard. Although the explosive strength of electrostatic spraying powder is relatively weak compared to explosive dust of metals such as aluminum and magnesium, the application environment of electrostatic spraying powder is usually in relatively closed spaces, close to personnel, and easier to come into contact with ignition sources, thereby increasing the severity of explosion of powder coatings. Therefore, in the actual process of electrostatic spraying, corresponding explosion prevention and control measures should be taken based on the explosion hazard levels of different powder coatings.

3.2. Ignition Sensitivity and Flame Propagation of Dust Clouds. The MITC and MIE of dust clouds describe the difficulty of dust combustion and are important characteristic parameters for evaluating dust ignition sensitivity.^{34,35} In order to compare and analyze the MIE of three powder coatings, the accurate value of MIE was calculated using eq 3³²

$$\log \text{MIE} = \log E_2 - I[E_2] \cdot \frac{(\log E_2 - \log E_1)}{(\text{NI} + I) \cdot [E_2] + 1} \quad (3)$$

In the formula, E_1 represents the highest energy value that has not been ignited for 10 consecutive times; E_2 represents the lowest energy value for 10 consecutive fires; $I[E_2]$ represents the number of ignition times at different concentrations under the ignition energy E_2 ; $(NI + I)[E_2]$ represents the total number of experiments at different concentrations.

Figure 10 shows the MITC and MIE test results of EPC, PPC, and APC. MITC values are found as follows: EPC > PPC >

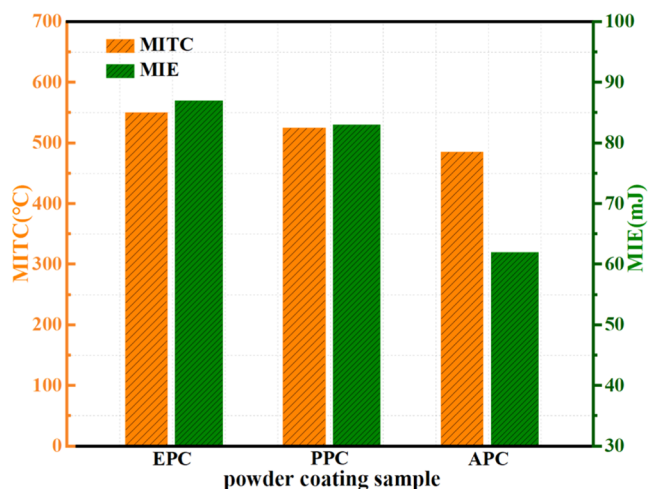


Figure 10. MITC and MIE of dust clouds.

APC, MIE value: EPC \approx PPC > APC, the MITC and MIE values of APC were significantly lower than those of the other two powders. The MITC and MIE of dust are related to the pyrolysis characteristics of powder coatings. Through thermogravimetric analysis, it was found that there is not much difference in the pyrolysis temperature of volatile matter among the three powder coating samples. Under the same conditions, the highest volatile content is in APC, and the lowest is in EPC. The volatile content is a key driving factor for dust ignition sensitivity, so APC can pyrolyze more volatile components under a certain high temperature or ignition energy, making them easier to ignite. Therefore, APC have the highest ignition sensitivity and are more prone to dust explosion accidents. In actual production processes, the hazards from electrostatic discharge should be considered.

It should be pointed out that the MITC and MIE values of the three powder coatings are greatly affected by the dispersion pressure during testing. Figures 11 and 12 show the trend of the MITC and MIE values of polyester and acrylic powder coatings under different dispersion pressures. As shown in Figure 11, the variation pattern of MITC under different concentrations is consistent, and overall, it decreases with increasing dispersion pressure. The dispersion pressure will have an impact on the dispersion degree and the injection amount of dust. As the dispersion pressure increases, more effective particles enter the furnace body, resulting in better dispersion of particles and fuller contact with air. The heat required to ignite the dust is lower. The reduction of the dispersion pressure is not conducive to the formation of dust clouds, and the agglomeration effect between particles leads to incomplete particle dispersion. The ignition of dust requires a higher ignition temperature to provide heat. As shown in Figure 12, as the dispersion pressure increases, the MIE values of both samples show a pattern of first decreasing and then increasing. When the dispersion pressure is low, the concentration of raised dust is low, particle aggregation is high, and dispersion is poor. The energy required to ignite dust particles is large. When the dispersion pressure is too high, the generated turbulence is strong and the spacing between dust particles is large. Moreover, the Hartmann tube is a semi-open pipeline, and some dust particles will escape to the outside of the pipeline. At this time, the dust concentration near the ignition electrode in the lower part of the pipeline is low, making ignition more difficult.

The flame propagation process of three powder coatings ignited in a vertical glass tube was recorded by using a high-speed camera. The microstructure and position changes of the flame front were systematically observed, and the average flame propagation speed was calculated based on the displacement amplitude of the flame front position at different time intervals. The moment when the flame begins to develop is defined as the zero moment of flame propagation, and the position of the highest point of the flame front from the ignition electrode is the position of the flame front. Figure 13 shows the trend of the flame front position and average flame propagation speed of the electrostatic spraying powder over time. The propagation process of the explosion flame of the three powders is generally similar. Compared to metal dust,³⁶ the development of the explosion flame of powder coatings is relatively slow, and the flame front propagates linearly upward. APC reaches the top of

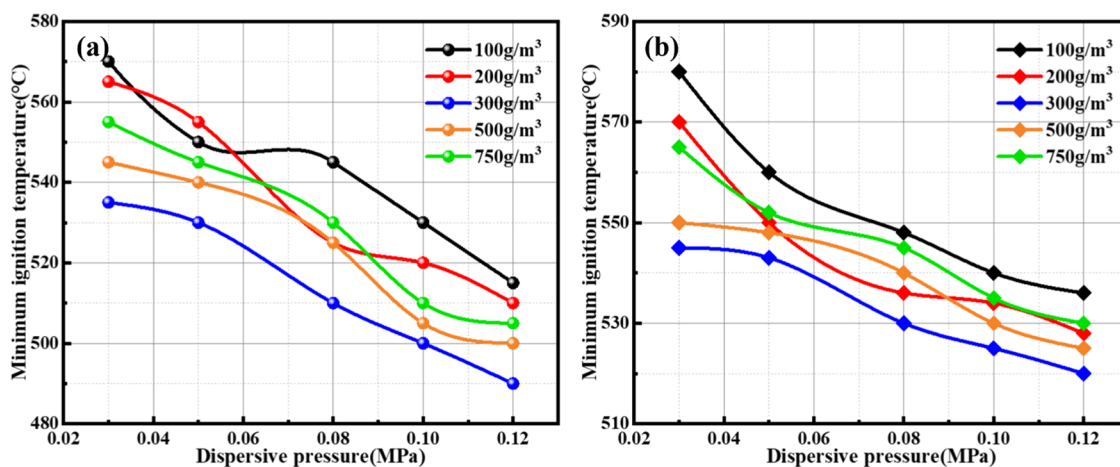


Figure 11. Relationship between MITC and dispersive pressure of dust clouds. (a) Polyester powder coating. (b) Acrylic powder coating.

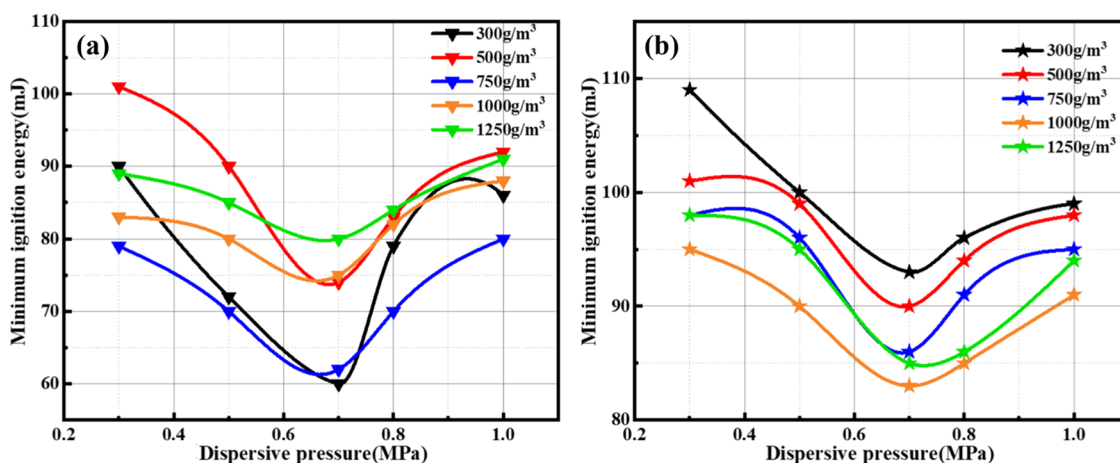


Figure 12. Relationship between MIE of dust clouds and dispersion pressure: (a) Polyester powder coating; (b) Acrylic powder coating.

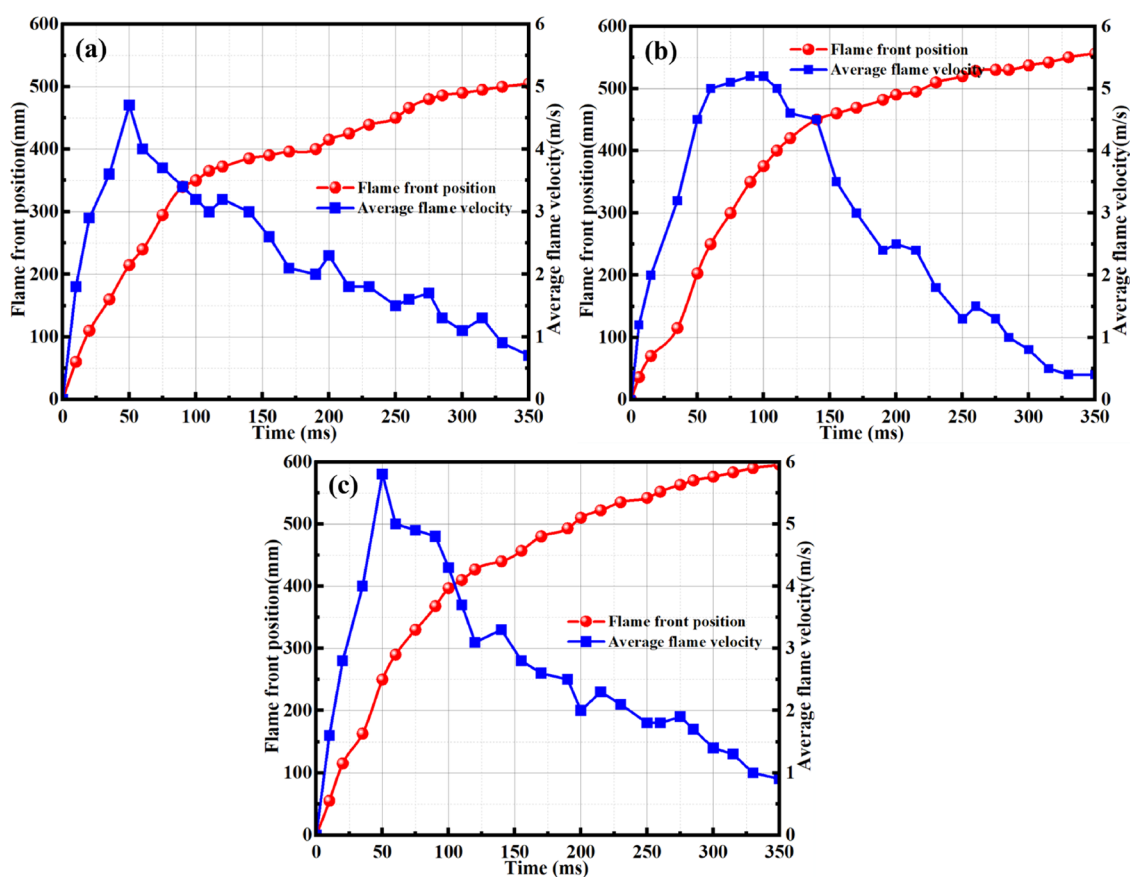


Figure 13. Changes in flame front position and propagation speed over time. (a) Epoxy powder coating. (b) Polyester powder coating. (c) Acrylic powder coating.

the pipeline at the fastest speed around 350 ms after ignition. The average flame propagation speed first increases and then decreases. The peak average flame velocity of APC reaches 5.9 m/s, which is more than 28% higher than that of EPC coating and 13% higher than that of PPC. This is because the low pyrolysis temperature and high volatile content of APC promote faster pyrolysis and precipitation of more volatile substances, accelerating the combustion reaction rate and flame propagation. In addition, during the propagation process, it was found that there was a certain degree of oscillation in the flame propagation speed. In the early stage of deflagration, the flame

propagation speed showed an approximate linear increase trend, and the speed quickly reached its peak. This is because the dust cloud in the experiment was formed by compressed air spraying, and the spraying airflow promoted the diffusion of dust, while also forming turbulence in the lower part of the pipeline, accelerating the combustion of dust, and promoting the rapid development and propagation of flames toward the upper part of the pipeline. In the later stage of deflagration, the flame front position continues to advance toward the top of the pipeline, but the flame propagation speed significantly decreases, and the flame speed shows slight fluctuations, which is caused by the

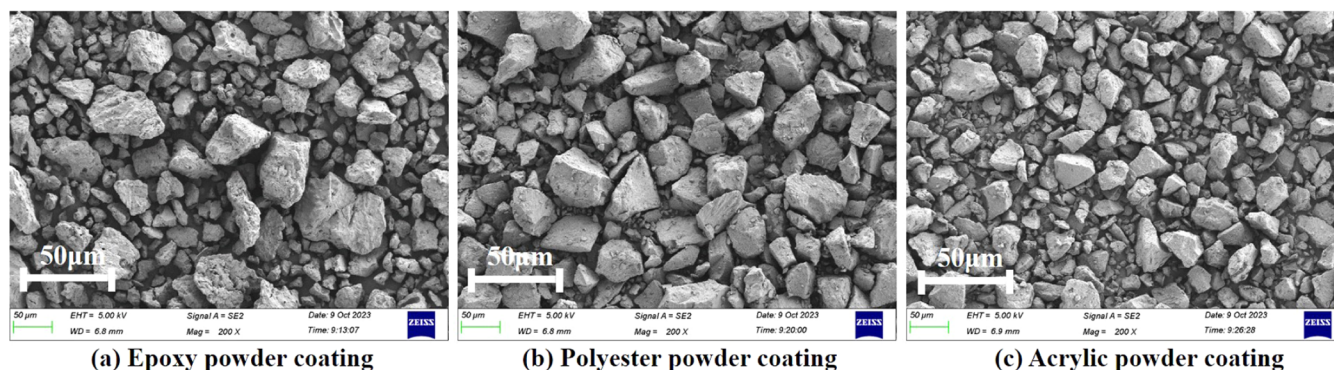


Figure 14. SEM images of electrostatic spraying powder before explosion.

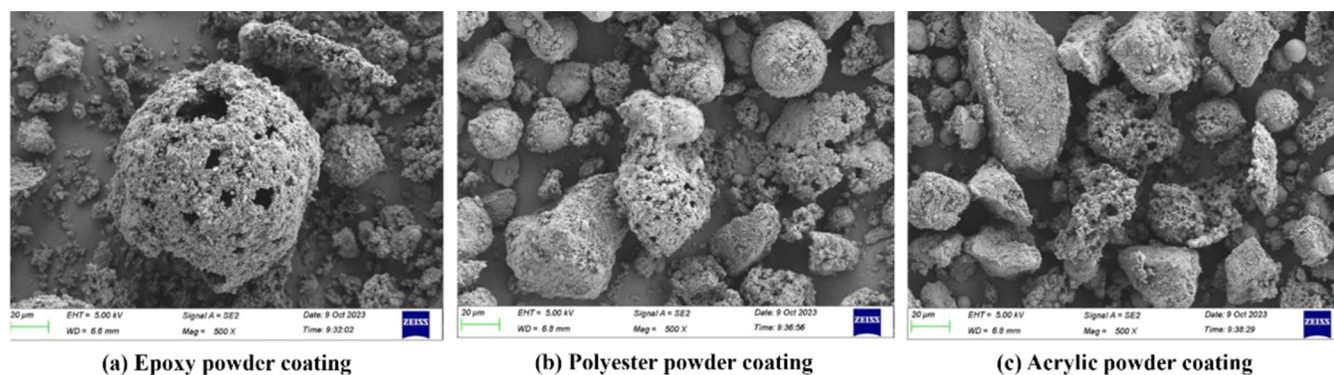


Figure 15. SEM images of electrostatic spraying powder after explosion (concentration of 1000 g/m^3).

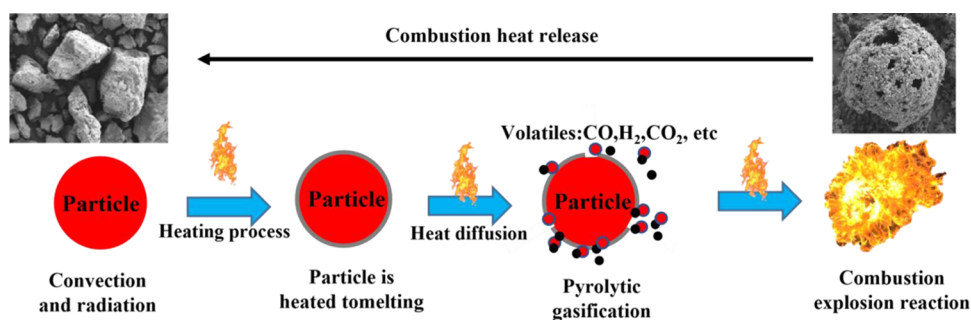


Figure 16. Explosion mechanism of electrostatic spraying powder.

feedback mechanism between the energy balance of particles in the preheating zone of the combustion process and the flame propagation speed.

3.3. Analysis of Microscopic Characteristics and Explosion Mechanism of Explosion Products. The products after dust explosion can serve as an important basis for analyzing the characteristics of dust explosion.³⁷ The microstructure characteristics of the three powder coating samples and their explosion products were characterized by SEM, and their explosion mechanisms were analyzed.

Figures 14 and 15, respectively, provide SEM images of the explosive products of three powder coating samples, EPC, PPC, and APC, before and after explosion at a concentration of 1000 g/m^3 . From the results of scanning electron microscopy, it can be seen that the particle shapes of the three powder coating samples are irregular with uneven particle size distribution. There are small amounts of small particles adhered to the large particles, and the surfaces of the particles are relatively smooth without obvious edges and corners. There is no visible pore

structure, and there is a small amount of particle aggregation in the finer powder samples. However, there are significant differences in the microscopic morphology characteristics of the dust particles after the explosion, and the explosive products exhibit melting characteristics and varying degrees of agglomeration. As shown in Figure 15a, after the explosion of the EPC, most of the dust particles became nearly spherical, and the agglomeration between the particles was very serious, resulting in a large number of visible pore structures, and some even turned into broken porous spherical shells.

As shown in Figure 15b,c, the particle adhesion and adsorption degree of explosive products from PPC and APC are relatively low and the surface of the particles is uneven. A large number of smaller particle residues are adsorbed in the large particles, resulting in a dense cluster like structure on the surface of the explosive products. Some of the explosive products are plate like lumps, but there is no obvious spherical shell structure. It can be seen that the combustion of electrostatic spraying powder coatings is incomplete, and it is

preliminarily speculated that the cross-linking curing reaction of powder coatings under explosive flame high temperature is one of the important reasons.

The explosion process of electrostatic spraying powder is relatively complex and is different from the diffusion flame propagation mode of surface oxidation and combustion of metal dust particles such as aluminum powder. Under the high-temperature effect of the explosion flame, powder coatings undergo cross-linking and solidification between particles, forming a dense and stable coating layer and experiencing varying degrees of agglomeration and solidification phenomena. Based on the results of scanning electron microscopy and previous research on the explosion mechanism of organic dust,^{38–40} a clear understanding of the explosion mechanism of electrostatic spraying powder can be obtained. As shown in Figure 16, the explosive development process of powder coating particles is concentrated in a three-phase system, where solid particles, molten particles, and combustible gases coexist. It undergoes a dynamic process of particle melting, cross-linking solidification, pyrolysis gasification, combustion, and extinction. First, due to the low melting point of powder coating particles, they will undergo melting after being heated to 180–220 °C. Then, smaller particles will begin to decompose and gasify, releasing various volatile substances such as CO, H₂, and CO₂ from within the particles. The combustible volatile gas will combine with oxygen on the surface of the particles for gas-phase combustion reaction. After the dust is ignited, it will continue to release combustible gas and release a large amount of heat, this further promotes pyrolysis. As the combustion reaction proceeds and the flame temperature increases, the agglomerated internal particles also begin to undergo pyrolysis and gasification, resulting in volume expansion and a sharp increase in internal stress.

At this stage, the resin and curing agent in the powder coating undergo cross-linking and curing reactions, forming a dense and stable coating on the surface of the particles and causing solidification and agglomeration, which can hinder the release of volatile matter and the entry of oxygen. The combustion reaction mainly occurs in the gas phase of the volatile/air mixture at a distance from the particle surface, resulting in incomplete combustion and the formation of more visible pore structures on the particles. When subjected to thermal stress and its explosive shock waves, fragmented spherical shell fragments are formed. The volatile content of EPC is relatively low, and the pore structure of explosive products is more developed, presenting a broken spherical shell structure. The explosive products of PPC and APC generally exhibit a porous cluster structure, which is mainly affected by the cross-linking and curing effects of the resin and curing agent in the powder coatings at high temperatures.

4. CONCLUSIONS

The explosion characteristics, ignition sensitivity, and flame propagation characteristics of three typical electrostatic spraying powders were studied by using a 20 L spherical explosion test device, a G-G furnace test device, and a Hartmann tube test device. The changes in the morphology of powder particles before and after the explosion were analyzed by electron microscopy, and the explosion mechanism of electrostatic spraying powders was explored. The following conclusions are drawn:

- (1) The P_{\max} of the three powder coatings is between 0.63 and 0.75 MPa, and the $(dP/dt)_{\max}$ is between 44.5 and 85.4 MPa/s. The P_{\max} and $(dP/dt)_{\max}$ of APC are the largest. The P_{\max} and $(dP/dt)_{\max}$ of all powders increased first and then decreased with the increase of mass concentration.
- (2) The MITC and MIE values of APC are significantly lower than those of the other two powders, and the volatile content of APC is the highest under the same conditions, which makes its flame spread the fastest. The flame propagation development of powder coating is relatively slow, the flame front spreads linearly upward, the average flame speed increases first and then decreases, and there is a certain degree of oscillation in the propagation process, which is related to the feedback mechanism between the energy balance of burning particles and the flame propagation speed.
- (3) The explosive development process of powder coating particles is concentrated in a three-phase system where solid particles, molten particles, and combustible gases coexist, undergoing a dynamic process of particle melting, cross-linking and solidification, pyrolysis and gasification, combustion, and extinction. The incomplete combustion of explosive products results in melting characteristics and varying degrees of agglomeration, with a large number of visible pore structures. The surface of explosive products presents a dense cluster like structure, suggesting that the cross-linking and curing reaction of powder coatings under high explosion flame temperatures is one of the important reasons.

■ AUTHOR INFORMATION

Corresponding Author

Xiangrui Wei – College of Safety and Environmental Engineering, Shandong University of Science and Technology, Qingdao, Shandong 266590, China; orcid.org/0000-0002-7978-7613; Email: relax_wxr@163.com

Authors

Xinxin Qin – College of Safety and Environmental Engineering, Shandong University of Science and Technology, Qingdao, Shandong 266590, China

Yansong Zhang – College of Safety and Environmental Engineering, Shandong University of Science and Technology, Qingdao, Shandong 266590, China; orcid.org/0000-0001-7312-7342

Jing Shi – College of Safety and Environmental Engineering, Shandong University of Science and Technology, Qingdao, Shandong 266590, China; orcid.org/0009-0003-7660-1793

Complete contact information is available at:

<https://pubs.acs.org/10.1021/acsomega.4c01724>

Author Contributions

The article was written through contributions of all authors. All authors have given approval to the final version of the article.

Notes

The authors declare no competing financial interest.

■ ACKNOWLEDGMENTS

This research was funded by the National Natural Science Foundation of China (51974179).

REFERENCES

- (1) Yang, K.; Zhai, M.; Pang, L.; Zhang, Y. Research on Risk Assessment Method of Dust Explosion in Electrostatic Powder Coating Firms. *J. Loss Prev. Process Ind.* **2023**, *86*, No. 105198.
- (2) Liu, W.; Bhuiyan, M. T. I.; Zhang, H.; Zhu, J. Boosting Flowability and Curing Reaction of Ultra-Fine Powder Coatings Using Facile-Fabrication $\text{Al}_2\text{O}_3/\text{C}_4\text{H}_6\text{N}_2$ Nanocomposite. *Prog. Org. Coat.* **2023**, *185*, No. 107836.
- (3) Pang, L.; Cao, J.; Xiao, Q.; Yang, K.; Shi, L. Explosion Propagation in a Dust Removal Pipeline under Dust Collector Explosion. *J. Loss Prev. Process Ind.* **2022**, *74*, No. 104662.
- (4) Zhang, Y.; Xu, K.; Liu, B.; Ge, J.; Geng, L.; Yan, K. Suppression Method of Industrial Al Alloy Powder Explosion in Dry and Humid Environment: A Low-Cost Intrinsic Safety Technology. *Adv. Powder Technol.* **2023**, *34* (9), No. 104131, DOI: 10.1016/j.apt.2023.104131.
- (5) Yan, K.; Meng, X.; Sun, H.; Qian, Y.; Shi, L.; Pan, Z.; Zhang, Y. Inhibition of Aluminum Powder Explosion by Sludge-Based Carbon Nanotubes/Phosphorus-Nitrogen Flame Retardant Composite Powder: Mechanism and Kinetic Model. *Adv. Powder Technol.* **2023**, *34* (9), No. 104110.
- (6) Jiang, H.; Bi, M.; Zhang, J.; Zhao, F.; Wang, J.; Zhang, T.; Xu, J.; Song, Y.; Gao, W. Explosion Characteristics and Mechanism of Aluminum-Reduced Graphene Oxide Composite Powder. *Powder Technol.* **2022**, *405*, No. 117545.
- (7) Zhang, Y.; Zhang, Y.; Shi, J.; Cao, M.; Wei, X.; Shi, L.; Wang, X. Experimental and Numerical Study on Suppressing Coal Dust Deflagration Flame with NaHCO_3 and MPP. *Fuel* **2024**, *358*, No. 130152.
- (8) Fengxiao, W.; Jinzhang, J.; Xiuyuan, T. Suppression of Methane Explosion in Pipeline Network by Carbon Dioxide-Driven Calcified Montmorillonite Powder. *Arab. J. Chem.* **2022**, *15* (10), No. 104126.
- (9) Fengxiao, W.; Jinzhang, J.; Xiuyuan, T. Performance and Mechanism of Bentonite in Suppressing Methane Explosions in a Pipeline Network. *Geomech. Geophys. Geo-Energy Geo-Resour.* **2023**, *9*, No. 13, DOI: 10.1007/s40948-023-00539-x.
- (10) Millogo, M.; Bernard, S.; Gillard, P. Combustion Characteristics of Pure Aluminum and Aluminum Alloys Powders. *J. Loss Prev. Process Ind.* **2020**, *68*, No. 104270, DOI: 10.1016/j.jlp.2020.104270.
- (11) Jiang, H.; Bi, M.; Zhang, T.; Shang, S.; Gao, W. A Novel Reactive P-Containing Composite with an Ordered Porous Structure for Suppressing Nano-Al Dust Explosions. *Chem. Eng. J.* **2021**, *416*, No. 129156.
- (12) Liu, J.; Meng, X.; Yan, K.; Wang, Z.; Dai, W.; Wang, Z.; Li, F.; Yang, P.; Liu, Y. Study on the Effect and Mechanism of $\text{Ca}(\text{H}_2\text{PO}_4)_2$ and CaCO_3 Powders on Inhibiting the Explosion of Titanium Powder. *Powder Technol.* **2022**, *395*, 158–167.
- (13) Huang, C.; Chen, X.; Yuan, B.; Zhang, H.; Dai, H.; He, S.; Zhang, Y.; Niu, Y.; Shen, S. Suppression of Wood Dust Explosion by Ultrafine Magnesium Hydroxide. *J. Hazard. Mater.* **2019**, *378*, No. 120723.
- (14) Liu, Y.; Zhang, Y.; Meng, X.; Yan, K.; Wang, Z.; Liu, J.; Wang, Z.; Yang, P.; Dai, W.; Li, F. Research on Flame Propagation and Explosion Overpressure of Oil Shale Dust Explosion Suppression by NaHCO_3 . *Fuel* **2022**, *314*, No. 122778.
- (15) Zhao, Q.; Li, Y.; Chen, X. Fire Extinguishing and Explosion Suppression Characteristics of Explosion Suppression System with N_2/APP after Methane/Coal Dust Explosion. *Energy* **2022**, *257*, No. 124767, DOI: 10.1016/j.energy.2022.124767.
- (16) Cao, Y.; Cheng, H.; Gu, N.; Ou, K.; Wang, Z.; Liu, Q.; Guan, R.; Fu, Q.; Sun, Y. Excellent Mechanical Durability of Superhydrophobic Coating by Electrostatic Spraying. *Mater. Chem. Phys.* **2023**, *301*, No. 127658.
- (17) Gheno, G.; Ganzerla, R.; Bortoluzzi, M.; Paganica, R. Accelerated Weathering Degradation Behaviour of Polyester Thermosetting Powder Coatings. *Prog. Org. Coat.* **2016**, *101*, 90–99.
- (18) Li, G.; Yuan, C.; Chen, B. Explosion Risk Evaluation during Production of Coating Powder. *J. Hazard. Mater.* **2007**, *149* (2), 515–517.
- (19) Bielawski, J. Fire and Explosion Hazards Associated with Electrostatic Powder Coating. *Zesz. Nauk. SGSP* **2020**, *75* (75), 23–36.
- (20) Di Benedetto, A.; Russo, P. Thermo-Kinetic Modelling of Dust Explosions. *J. Loss Prev. Process Ind.* **2007**, *20* (4–6), 303–309.
- (21) Velickova, E.; Stroh, P.; Velicka, R. Assessment of the Normative Requirements for Ensuring the Safety of Powder Coating Booths in Terms of the Risk of Explosion. *Trans. VSB-Tech. Univ. Ostrava, Saf. Eng. Ser.* **2017**, *10* (2), 33–40, DOI: 10.1515/tvsbses-2015-0011.
- (22) Eckhoff, R. K.; Pedersen, G. H.; Arvidsson, T. Ignitability and Explosibility of Polyester/Epoxy Resins for Electrostatic Powder Coating. *J. Hazard. Mater.* **1988**, *19* (1), 1–16.
- (23) Castellanos, D.; Carreto-Vazquez, V. H.; Mashuga, C. V.; Trottier, R.; Mejia, A. F.; Mannan, M. S. The Effect of Particle Size Polydispersity on the Explosibility Characteristics of Aluminum Dust. *Powder Technol.* **2014**, *254*, 331–337.
- (24) Xu, G.; Wang, S.; Cai, X.; Mei, J.; Zou, H.; Zhang, L.; Qian, H. Study on Characteristics, Hydrogen-Rich Gas, Bio-Oil Production, and Process Optimization of Co-Pyrolysis of Sewage Sludge and Wheat Straw. *Case Stud. Therm. Eng.* **2023**, *45*, No. 102888.
- (25) Raza, M.; Abu-Jdayil, B. Synergic Interactions, Kinetic and Thermodynamic Analyses of Date Palm Seeds and Cashew Shell Waste Co-Pyrolysis Using Coats–Redfern Method. *Case Stud. Therm. Eng.* **2023**, *47*, No. 103118.
- (26) Wei, X.; Zhang, Y.; Wu, G.; Zhang, X.; Zhang, Y.; Wang, X. Study on Explosion Suppression of Coal Dust with Different Particle Size by Shell Powder and NaHCO_3 . *Fuel* **2021**, *306*, No. 121709.
- (27) Zhang, Y.; Wu, G.; Cai, L.; Zhang, J.; Wei, X.; Wang, X. Study on Suppression of Coal Dust Explosion by Superfine NaHCO_3 /Shell Powder Composite Suppressant. *Powder Technol.* **2021**, *394*, 35–43.
- (28) Yuan, Q.; Bu, Y.; Amyotte, P.; Chen, H.; Li, C.; Li, G.; Dong, Z.; Yuan, C. Effect of Particle Size Polydispersity on the Minimum Ignition Temperature of PMMA Dust Clouds. *Powder Technol.* **2022**, *410*, No. 117858.
- (29) Liu, H.; Chen, H.; Zhang, X.; Hu, Y.; Fan, C. Effects of Different Factors on the Minimum Ignition Temperature of the Mixed Dust Cloud of Coal and Oil Shale. *J. Loss Prev. Process Ind.* **2019**, *62*, No. 103977.
- (30) Shi, W.; Chen, J.; Liu, Y.; Li, N.; Zhang, Y.; Yang, J.; Han, J.; Li, R. Study on the Preparation of Novel $\text{NiB}/\text{H}\beta\text{-Al}_2\text{O}_3$ Micro-Mesoporous Suppressant and Its Inhibition Mechanism of Coal Dust Explosion Flame. *J. Loss Prev. Process Ind.* **2023**, *83*, No. 105072.
- (31) Qiu, D.; Dong, Z.; Liu, L.; Huang, C.; Yue, Y.; Zhang, G.; Hao, L.; Chen, X. Preparation of Modified Fly Ash-Based, Core–Shell Inhibitor and Its Effect on Suppression of Al-Mg Alloy Dust Explosion. *Chem. Eng. J.* **2023**, *468*, No. 143741, DOI: 10.1016/j.cej.2023.143741.
- (32) Castells, B.; Amez, I.; León, D.; García-Torrent, J. Coloured Powder Potential Dust Explosions. *J. Loss Prev. Process Ind.* **2023**, *83*, No. 105014, DOI: 10.1016/j.jlp.2023.105014.
- (33) Wang, C.; Dong, X.; Ding, J.; Nie, B. Numerical Investigation on the Spraying and Explosibility Characteristics of Coal Dust. *Int. J. Min., Reclam. Environ.* **2014**, *28* (5), 287–296.
- (34) Zhang, J.; Sun, L.; Sun, T.; Zhou, H. Study on Explosion Risk of Aluminum Powder under Different Dispersions. *J. Loss Prev. Process Ind.* **2020**, *64*, No. 104042.
- (35) Cheng, Y. C.; Liao, S. W.; Alauddin, M.; Amyotte, P.; Shu, C. M. Redefining of Potential Dust Explosion Risk Parameters for Additives in the Petrochemical Manufacturing Process. *Process Saf. Environ. Prot.* **2023**, *169*, 472–480.
- (36) Wang, Z.; Meng, X.; Liu, J.; Zhang, Y.; Wang, Z.; Dai, W.; Yang, P.; Liu, Y.; Li, F.; Yan, K. Flame Propagation Behaviours and Explosion Characteristics of Al-Mg Alloy Dust Based on Thermodynamic Analysis. *Powder Technol.* **2022**, *406*, No. 117559.
- (37) Liu, B.; Zhang, Y.; Meng, X.; Chen, J.; Wang, J.; Wang, X.; Zhang, Y. Study on Explosion Characteristics of the Inert Substances at Longkou Oil Shale of China. *Process Saf. Environ. Prot.* **2020**, *136*, 324–333, DOI: 10.1016/j.psep.2019.12.033.
- (38) Zhang, G.; Zhang, Y.; Huang, X.; Gao, W.; Zhang, X. Effect of Pyrolysis and Oxidation Characteristics on Lauric Acid and Stearic Acid Dust Explosion Hazards. *J. Loss Prev. Process Ind.* **2020**, *63*, No. 104039, DOI: 10.1016/j.jlp.2019.104039.

(39) Zhang, X.; Gao, W.; Yu, J.; Zhang, Y.; Zhang, J.; Huang, X.; Chen, J. Effect of Flame Propagation Regime on Pressure Evolution of Nano and Micron PMMA Dust Explosions. *J. Loss Prev. Process Ind.* **2020**, *63*, No. 104037, DOI: [10.1016/j.jlp.2019.104037](https://doi.org/10.1016/j.jlp.2019.104037).

(40) Zhang, X.; Gao, W.; Yu, J.; Zhang, Y.; Chen, H.; Huang, X. Flame Propagation Mechanism of Nano-Scale PMMA Dust Explosion. *Powder Technol.* **2020**, *363*, 207–217.